Journal of
Composites Science

MDPI

Article

Enhanced Reverse-Engineering Method for Accurately Predicting Lamina Properties in Laminated Composites via Combined Static and Dynamic Finite Element Simulations

Mun-Young Hwang [1], Jeong Hun Park [1], Jongho Song [1], Soo Woong Hwang [2], Hun Hee Kang [3] and Hyun Chul Lee [1,*]

[1] Multi-Material Research Center, Korea Automotive Technology Institute, 55 Jingoksandanjungang-ro, Gwangsan-gu, Gwangju 62465, Republic of Korea; myhwangl@katech.re.kr (M.-Y.H.)
[2] Moodng Co., Ltd., 297 Pyung Dong Sandan-ro, Gwangsan-gu, Gwangju 62414, Republic of Korea; sw@moodng.com
[3] NK Alkenz Co., Ltd., R&D Team, 91 Gasan-ro, Jinyeong-eup, Gimhae-si 50849, Republic of Korea; khh@alkenz.com
* Correspondence: hclee@katech.re.kr

Abstract: This study aims to ascertain the material characteristics that are intrinsic to the prepreg layer within a laminated composite structure. The elastic modulus of the lamina, a primary determinant of composite structural behavior, is the focal point of this analysis. This parameter has been assessed by employing reverse-engineering techniques on a composite composed of sequentially stacked prepregs. The investigation entailed simulating the behavior of the composite under static loads and conducting modal analyses to reflect both static and dynamic conditions. The findings indicate that the elastic modulus values derived from combined tensile and modal analysis simulations exhibit superior accuracy compared to those obtained through tensile simulation alone. Specifically, the maximum prediction error for E_1 (the tensile-direction elastic modulus of one lamina sheet) decreased from 1.17% to 0.28%, and that of E_2 (the transverse-direction elastic modulus of one lamina sheet) decreased from 12.01% to 7.30%. Further simulations incorporating fabrication error variances underscored the critical nature of precise E_2 analysis. The proposed methodology evidenced a more accurate assessment of E_2, underscoring its potential to enhance the reverse-engineering process in composite material design.

Keywords: finite element analysis; laminate; laminate theory; multi-mechanism modeling

check for updates

Citation: Hwang, M.-Y.; Park, J.H.; Song, J.; Hwang, S.W.; Kang, H.H.; Lee, H.C. Enhanced Reverse -Engineering Method for Accurately Predicting Lamina Properties in Laminated Composites via Combined Static and Dynamic Finite Element Simulations. *J. Compos. Sci.* **2023**, *7*, 518. https://doi.org/10.3390/jcs7120518

Academic Editor: Salvatore Brischetto

Received: 11 November 2023
Revised: 30 November 2023
Accepted: 14 December 2023
Published: 15 December 2023

Copyright: © 2023 by the authors. Licensee MDPI, Basel, Switzerland. This article is an open access article distributed under the terms and conditions of the Creative Commons Attribution (CC BY) license (https://creativecommons.org/licenses/by/4.0/).

1. Introduction

Fiber-reinforced composite materials are increasingly recognized as an advantageous option for lightweight design due to their superior specific strength and flexibility relative to traditional metallic materials. Extensive research has focused on developing components utilizing fiber-reinforced composites and the methodologies for their analysis. For instance, Mahmood et al. [1] innovated a unidirectional E-glass fiber leaf spring, achieving an 80% weight reduction. Similarly, Choi et al. [2] validated using finite element models for part structures by aligning simulation outcomes with experimental results.

Central to these developments is the foundational technique of designing composites from scratch. A recurring challenge in composite material development is the occasional lack of precise material data concerning the laminae within composite structures. To mitigate this, many manufacturers have resorted to reverse-engineering techniques. This approach deduces the physical properties of each lamina by examining the behavior of the entire structure. Predominantly, prior research [3–8] has detailed procedures for creating accurate computer-aided design models via 3D scanning, while investigations into material selection through reverse engineering [9] have been conducted, albeit limited to isotropic substances.

Applying traditional reverse-design methods to composites, which are inherently anisotropic and vary in their material elastic modulus, layer thickness, lamination angle, and stacking sequence, presents significant challenges [10]. The accurate analysis of materials in laminated composites requires iterative experimental procedures, such as cyclic load tests, cross-sectional evaluations, and fiber volume ratio assessments. Moreover, to achieve dependable outcomes, extensive specimen testing is essential, a process that is not only costly but also fraught with variability at the macroscale due to the complexity of managing microscale test parameters (e.g., lamination angle, order, and the bonding of fibers to resins) [11,12]. Therefore, reverse engineering using only experimental approaches is preferred.

One of the paramount challenges in the reverse engineering of composites lies in characterizing the fabricated materials from the microstructural attributes of their constituents. Many studies have employed ASTM standard tests at the lamina level to elucidate the elastic properties of laminated composites. However, these experiments often estimate in-plane properties and out-of-plane shear moduli—primarily influenced by the resin—thus diminishing the precision of the material property data. In reverse engineering, a range of standardized tests are utilized for accurate material property determination, such as the fiber-direction Young's modulus (ASTM D3379) [13] and the tensile strength of the resin (ASTM D638) [14]. Consequently, a reverse-design technique [15,16], grounded in classical laminated plate theory (CLPT) [17], has been formulated. This technique utilizes inverse calculations predicated on mixture rules, yielding high accuracy in fiber-direction property predictions, albeit less so in the matrix direction.

To address these limitations, a multiscale method has been adopted. The method, referenced in prior and current research, leverages the macroscopic dynamic response of laminated composites to infer the elastic properties of both the composite and the individual laminae.

The principal approach of this investigation was to decipher the elastic properties of laminae within laminated composites through their macroscopic modal characteristics, as evidenced by various studies [18–21]. These methods commonly employ specialized algorithms to refine error margins in dynamic property-based finite element calculations. In our work, the lamina's elastic property estimates were refined by using a genetic algorithm, proposing an advanced methodology that utilizes modal analysis simulations predicated on dynamic characteristics to offset the limitations that are inherent to CLPT-based inverse calculations. The flow of this study, to predict the lamina material properties used in parts from laminated composites through reverse engineering, is shown in Figure 1. The ultimate goal of this study is to help designers select materials by minimizing the number of physical tests when designing parts for composite materials.

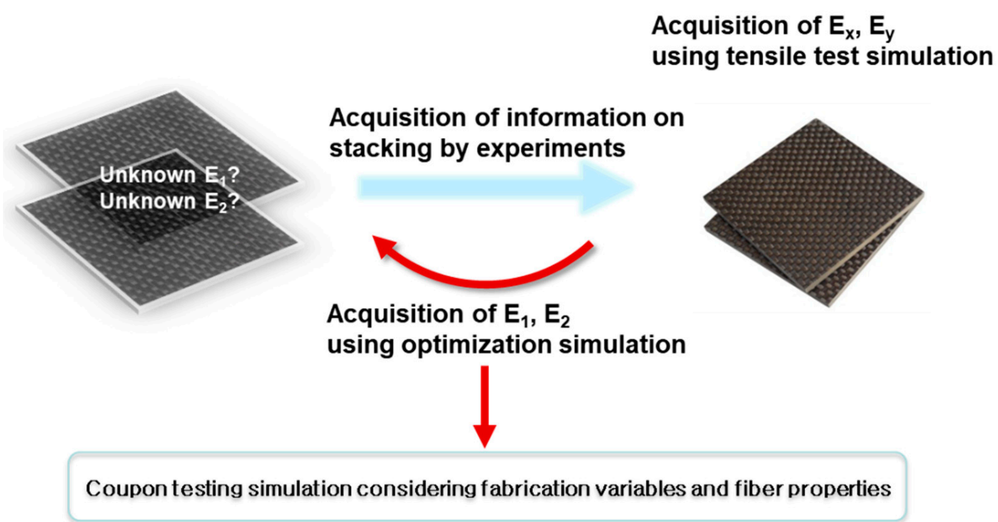

Figure 1. Fundamental concept underlying the simulation conducted in this study.

This analysis, considering dynamic properties, allows for the selection of cases where the fiber direction and matrix physical properties are definitive. The methodology surmounts the deficits of prior reverse-engineering approaches and accounts for the stack orientation of internal fibers. The commercial software ANSYS Composite PrePost (ANSYS ACP, Version R17.2) was utilized to develop the 3D finite element model (FEM), incorporating fiber details. Various tensile simulations were iterated to prognosticate material properties. This proposed method permits an intuitive verification of predictive results via finite element simulations, with the reliability of these predictions corroborated through a retrospective comparison with established research findings [15].

2. Modeling Approach for Predicting Lamina Properties

The traditional process of reverse engineering in composite structures relies on the characterization of lamina properties from testing specimens sourced from finished composites. However, these properties may not be accurate due to variations in fabrication parameters and lamination details. Thus, a method that accurately reflects the attributes of laminated composites is essential for effective reverse engineering. This research aims to deduce material properties by harnessing the dynamic response data of a laminated composite. This dynamic response is a reference acquired through the numerical analysis of a standard structure. Utilizing this reference, the effective elastic properties of the lamina are computed at the mesoscopic level alongside the macroscopic scale's natural frequencies of the multi-layered plate.

The three-dimensional constitutive equations in Equation (1) engage with stress–strain relationships, whereas laminate constitutive equations concern mid-plane strains and curvatures. The laminate construction equation, derived from the definition of stress, integrates these relationships. In 3D elasticity, stress is distributed at each material point. Concurrently, stress resultants—integral sums of stress components over the element's thickness—impose load on an element [22].

$$
\begin{gathered}
\begin{Bmatrix} N_x \\ N_y \\ N_{xy} \end{Bmatrix} = \sum_{k=1}^{N} \int_{z_{k-1}}^{z_k} \begin{Bmatrix} \sigma_x \\ \sigma_y \\ \sigma_{xy} \end{Bmatrix}^k dz \\
\begin{Bmatrix} V_y \\ V_x \end{Bmatrix} = \sum_{k=1}^{N} \int_{z_{k-1}}^{z_k} \begin{Bmatrix} \sigma_{yz} \\ \sigma_{xz} \end{Bmatrix}^k dz \\
\begin{Bmatrix} M_x \\ M_y \\ M_{xy} \end{Bmatrix} = \sum_{k=1}^{N} \int_{z_{k-1}}^{z_k} \begin{Bmatrix} \sigma_x \\ \sigma_y \\ \sigma_{xy} \end{Bmatrix}^k dz
\end{gathered} \tag{1}
$$

where M_x, M_y, M_{xy} are moments per unit length in the coordinates. N_x, N_y, N_{xy} are in-plane forces per unit length in the coordinates. V_x, V_y are shear forces per unit length in the coordinates. Index x, y means the principle direction of an element in the global coordinates. N is the number of laminae. z_{k-1} and z_k are the coordinates of the bottom and top surfaces of the k-th lamina, respectively. By replacing the plane-stress version of the 3D constitutive equations in the element's local coordinates at each lamina and then performing integration, the following is achieved:

$$\begin{Bmatrix} N_x \\ N_y \\ N_{xy} \\ M_x \\ M_y \\ M_{xy} \end{Bmatrix} = \begin{bmatrix} A_{11} & A_{12} & A_{16} & B_{11} & B_{12} & B_{16} \\ A_{12} & A_{22} & A_{26} & B_{12} & B_{22} & B_{26} \\ A_{16} & A_{26} & A_{66} & B_{16} & B_{26} & B_{66} \\ B_{11} & B_{12} & B_{16} & D_{11} & D_{12} & D_{12} \\ B_{12} & B_{22} & B_{26} & D_{12} & D_{22} & D_{26} \\ B_{16} & B_{26} & B_{66} & D_{16} & D_{26} & D_{66} \end{bmatrix} \begin{Bmatrix} \epsilon_x \\ \epsilon_y \\ \gamma_{xy} \\ \kappa_x \\ \kappa_y \\ \kappa_{xy} \end{Bmatrix} \tag{2}$$

$$\begin{Bmatrix} V_x \\ V_y \end{Bmatrix} = \begin{bmatrix} H_{44} & H_{45} \\ H_{45} & H_{55} \end{bmatrix} \begin{Bmatrix} \gamma_{yz} \\ \gamma_{xz} \end{Bmatrix}$$

where

$$A_{ij} = \sum_{k=1}^{N} \left(\overline{Q}_{ij}\right)_k t_k;\ i,j = 1,2,6 \tag{3}$$

$$B_{ij} = \sum_{k=1}^{N} \left(\overline{Q}_{ij}\right)_k t_k \overline{z}_k;\ i,j = 1,2,6 \tag{4}$$

$$D_{ij} = \sum_{k=1}^{N} \left(\overline{Q}_{ij}\right)_k \left(t_k \overline{z}_k^2 + \frac{t_k^3}{12}\right);\ i,j = 1,2,6 \tag{5}$$

$$H_{ij} = \frac{5}{4} \sum_{k=1}^{N} \left(\overline{Q}_{ij}^*\right)_k \left[t_k - \frac{4}{t^2}\left(t_k \overline{z}_k^2 + \frac{t_k^3}{12}\right)\right];\ i,j = 4,5 \tag{6}$$

where $\left(\overline{Q}_{ij}\right)_k$ denotes the coefficient of the laminate coordinates of the plane-stress stiffness matrix for the k-th lamina, t_k denotes the thickness of the k lamina, and $\overline{z}_k$ denotes the coordinate of the middle surface of the k lamina. The coefficients A_{ij},D_{ij},B_{ij}, and H_{ij} represent the in-plane stiffness of the laminate, bending stiffness, bending–extension coupling, and intralaminar shear stiffness, respectively. These coefficients can be calculated using Equations (3)–(6) and are implemented in widely available software packages such as ANSYS ACP R17.2.

The stress–strain relationship observed in references [23,24] was derived from the relationship of the orthotropic layers. Therefore, the stresses at all the locations in the k layer are

$$\begin{Bmatrix} \sigma_1 \\ \sigma_2 \\ \tau_{23} \\ \tau_{13} \\ \tau_{12} \end{Bmatrix} = \begin{bmatrix} Q_{11} & Q_{12} & 0 & 0 & 0 \\ Q_{21} & Q_{22} & 0 & 0 & 0 \\ 0 & 0 & Q_{44} & 0 & 0 \\ 0 & 0 & 0 & Q_{55} & 0 \\ 0 & 0 & 0 & 0 & Q_{66} \end{bmatrix} \begin{Bmatrix} \varepsilon_1 \\ \varepsilon_2 \\ \gamma_{23} \\ \gamma_{13} \\ \gamma_{12} \end{Bmatrix} \tag{7}$$

where σ_i, τ_{ij}, ε_i, and γ_{ij} are the stress component, the shear stress component, the strain component, and the shear strain component in the tensor notation.

Index 1 represents the direction of the fibers, index 2 represents the direction perpendicular to the fiber orientation at the layer surface, and indices 12, 13, and 23 represent the shear directions in the local coordinates of the element. Q_{ij} is the elastic property of the layer. As explained in [25], to apply the principle of virtual work, it is necessary to convert the stresses and strains from the principal coordinates to local coordinates (x and y) as follows:

$$\begin{Bmatrix} \sigma_1 \\ \sigma_2 \\ \tau_{23} \\ \tau_{13} \\ \tau_{12} \end{Bmatrix} = \begin{bmatrix} cos^2\theta & sin^2\theta & 0 & 0 & 2sin\theta cos\theta \\ sin^2\theta & cos^2\theta & 0 & 0 & -2sin\theta cos\theta \\ 0 & 0 & cos\theta & -sin\theta & 0 \\ 0 & 0 & sin\theta & cos\theta & 0 \\ -sin\theta cos\theta & sin\theta cos\theta & 0 & 0 & -sin^2\theta + cos^2\theta \end{bmatrix} \begin{Bmatrix} \sigma_x \\ \sigma_y \\ \tau_{yz} \\ \tau_{xz} \\ \tau_{xy} \end{Bmatrix} \tag{8}$$

$$\begin{Bmatrix} \varepsilon_1 \\ \varepsilon_2 \\ \gamma_{23} \\ \gamma_{13} \\ \gamma_{12} \end{Bmatrix} = \begin{bmatrix} cos^2\theta & sin^2\theta & 0 & 0 & sin\theta cos\theta \\ sin^2\theta & cos^2\theta & 0 & 0 & -sin\theta cos\theta \\ 0 & 0 & cos\theta & -sin\theta & 0 \\ 0 & 0 & sin\theta & cos\theta & 0 \\ -2sin\theta cos\theta & 2sin\theta cos\theta & 0 & 0 & -sin^2\theta + cos^2\theta \end{bmatrix} \begin{Bmatrix} \varepsilon_x \\ \varepsilon_y \\ \gamma_{yz} \\ \gamma_{xz} \\ \gamma_{xy} \end{Bmatrix} \tag{9}$$

θ is the fiber angle in the local coordinates of the element, which may differ at each point of the lamina in the laminated composite. The innovative aspect of this research lies in accounting for the variations in fiber orientation and their effects. In the context of this study, when applying the principle of virtual work, the local stresses at the surface of each layer, as delineated in Equation (9), are presumed to be uniform. This uniformity does not extend to the general points within each layer, where local stresses diverge. To address this, a conceptual operation involving inertia and strength parameters are introduced, applying the principles of this hypothetical task to derive the motion equation. This equation takes the following form [26]:

$$\begin{bmatrix} M^{11} & 0 & 0 & 0 & 0 \\ 0 & M^{22} & 0 & 0 & 0 \\ 0 & 0 & M^{33} & M^{34} & M^{35} \\ 0 & 0 & M^{43} & M^{44} & 0 \\ 0 & 0 & M^{53} & 0 & M^{55} \end{bmatrix} \begin{Bmatrix} \ddot{q}_u(t) \\ \ddot{q}_v(t) \\ \ddot{q}_\omega(t) \\ \ddot{q}_{\phi_x}(t) \\ \ddot{q}_{\phi_y}(t) \end{Bmatrix} + \begin{bmatrix} K^{11} & K^{12} & 0 & 0 & 0 \\ K^{21} & K^{22} & 0 & 0 & 0 \\ 0 & 0 & K^{33} & K^{34} & K^{35} \\ 0 & 0 & K^{43} & K^{44} & K^{45} \\ 0 & 0 & K^{53} & K^{54} & K^{55} \end{bmatrix} \begin{Bmatrix} q_u(t) \\ q_v(t) \\ q_\omega(t) \\ q_{\phi_x}(t) \\ q_{\phi_y}(t) \end{Bmatrix} = \begin{Bmatrix} \varepsilon_1 \\ \varepsilon_2 \\ \gamma_{23} \\ \gamma_{13} \\ \gamma_{12} \end{Bmatrix} \tag{10}$$

where M and K are the mass and stiffness submatrices, respectively, and are constants. Assuming the second derivative of the generalized displacement over time to be $\ddot{q}(t) = -\omega^2 q(t)$, Equation (10) becomes an eigenvalue problem: here, the eigenvalues are squares of the eigenfrequencies, and the eigenvectors define their mode forms.

The laminate's constitutive matrices—A, B, D, and H—encapsulate its definition, establishing a relationship between the generalized forces and moments with the corresponding generalized strains and curvatures. These matrices enable the computation of laminate properties predicated on the laminate stacking sequence and the individual lamina properties. Additionally, the elastic modulus of each lamina is extrapolated from the corresponding constitutive matrix, and the modal frequency of each element's shape is ascertained.

In typical reverse analyses of laminated composites, it is imperative to calculate the stress and strain distributions for each lamina within the laminate. The true laminate stacking order is then inputted into the analysis software, where the elastic properties, thickness, and fiber orientation for each lamina are specified and computed. However, the present study deviates from this norm by estimating the lamina properties of the laminated composite directly from the tensile simulation results, utilizing the known laminate stacking sequence and previously derived constitutive matrices.

3. Procedure for Predicting Lamina Properties

The ultimate aim of the outlined procedure is to produce a composite component that meets the design requirements in strength by selecting an apt composite material. The proposed inverse design methodology for predicting lamina properties is delineated into five stages, as illustrated in Figure 2.

Initially, specimen retrieval from the final product is essential for benchmarking to evaluate the lamina sequence, orientation, and thickness—crucial steps in reverse engineering for product design that significantly enhance prediction accuracy. Techniques such as burnout tests (to analyze lamina post-resin combustion) and optical inspections of the cross-section [27,28] are employed to ascertain lamination details precisely. However, this study operates on the premise that these stacking data are accurately obtainable, thus concentrating on CAE-based techniques exclusively for predicting lamina properties within laminated composites.

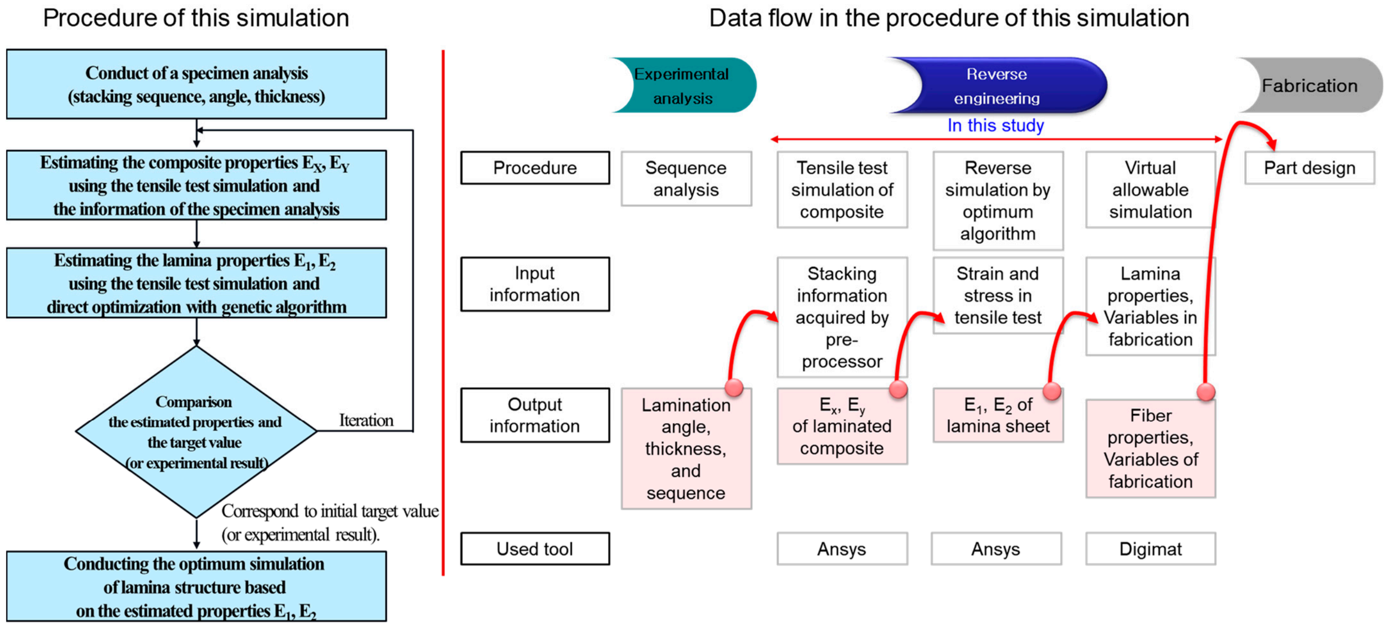

Figure 2. The simulation procedure and data flow in this study.

The second phase involves predicting the elastic modulus components, E_X and E_Y, in the Cartesian coordinate plane of the laminated composite derived from tensile simulations coupled with specimen analysis data.

Subsequently, the third stage predicts the lamina's elastic modulus components, E_1 and E_2, along the Cartesian axes through tensile simulation and a direct optimization technique utilizing a genetic algorithm.

In the fourth stage, the calculated values of E_X (the tensile-direction elastic modulus of the laminated composite) and E_Y (the transverse-direction elastic modulus of the laminated composite) are juxtaposed from both the E_1 and E_2 estimations and tensile simulations of composite specimens. The results of this comparison authenticate the predicted elastic modulus of the lamina and determine the feasibility of advancing to the subsequent step. Concurrently, an FEM is constructed, factoring in variables that are indicative of the fabrication process of the laminated composite, equipped with the predicted elastic properties E_1 and E_2. Tensile simulations are then executed using this model to statistically ascertain the potential range of properties within the selected lamina.

The final step optimizes the lamination information based on the predicted values of E_1 and E_2. This optimization necessitates a case-by-case approach due to the variability of environmental and structural shape factors. Hence, this research targets a methodology for projecting lamina properties from part-derived specimens.

3.1. Tensile Simulation for Predicting E_X and E_Y of the Laminated Composite

To predict the elastic modulus components, E_X and E_Y, of laminated composites, tensile and modal simulations were conducted using ANSYS, an established finite element analysis software. The three-dimensional modeling of the composite structure was facilitated by the SOLID 185 element, featuring eight nodes with three degrees of freedom (X, Y, and Z) at each node. The simulation scenarios were aligned with the actual tensile test conditions. As depicted in Figure 3, the specimen region was immobilized using a fixture, with load conditions that induced deformation at 2 mm/min in the X-direction, as per ASTM D3039 [29] standards for the tensile testing of composite materials. In Figure 3, "Fixed support" refers to the part fixed by a jig in the specimen in the actual tensile test.

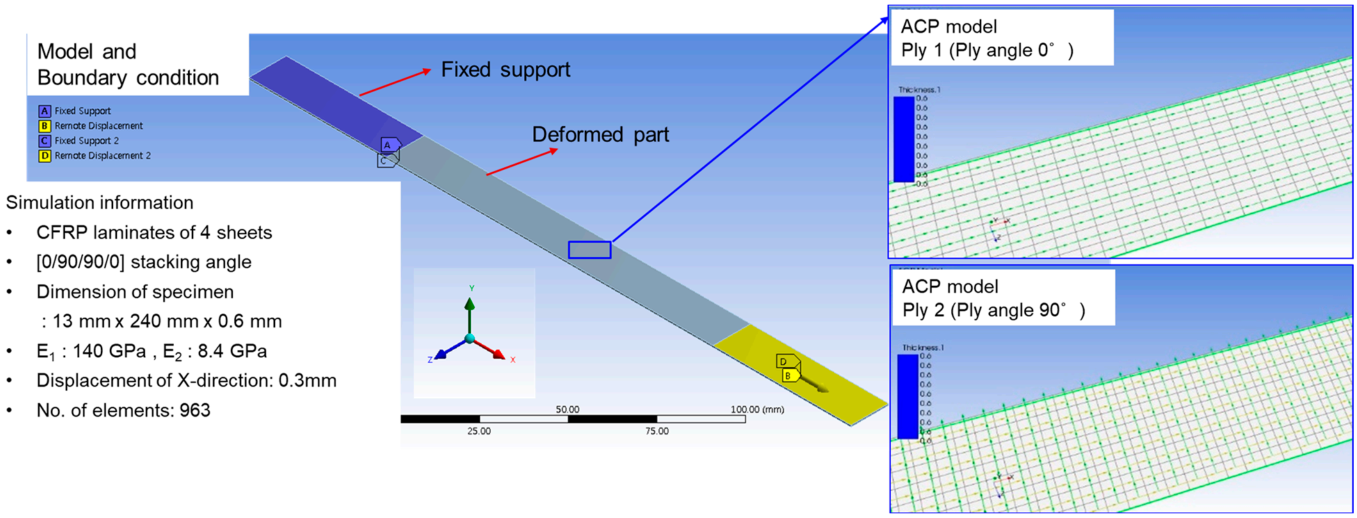

Figure 3. Schematic of tensile simulation and modal test simulation for predicting lamina properties of laminated composite.

Furthermore, the modal simulation settings replicated those of the actual frequency response function test conditions, ensuring that each specimen was fixed, and the anisotropic nature of the fibers was accounted for by setting scenarios where vibrations could occur in multiple directions. Only a linear analysis was employed to optimize the analysis duration and simplify the process, excluding material failure considerations at this juncture. Loads were validated against specimen deformation, and data were recorded over time to capture the evolution of tensile stress with strain incrementation—though the material's maximum tensile strength was not simulated. The ultimate goal of simulation in this study is to help fabricate composite parts composed of fibers and matrix materials with appropriate stiffness to meet design goals. For this purpose, the preliminary step is to acquire a specimen from a benchmarking part and analyze the stacking information of the acquired specimen. These methods for accurately analyzing stacked information are not within the scope of this study. The methods include burnout testing (burning the base material in composite materials and analyzing the information in the fiber layer) and optical observation of the cut surface. The assumption of this study is that the stacking information of the specimens can be accurately analyzed through these methods. Therefore, the scope of this study is technology to predict the properties of lamina in laminated composites using only CAE-based methods. Additionally, because the goal is this study is guidelines to help engineers select appropriate materials while minimizing actual physical testing, strength was not considered in order to minimize test variables during the reverse-engineering process.

In modal simulations, the FEM's validity extended up to the sixth frequency mode, providing insights into the specimen's varied modal shapes in relation to fiber orientation. This model, constructed with precise lamina order, angle, and thickness considerations using ANSYS ACP, also incorporated the stacking sequence. Initial material property values were based on a general-grade fiber material from the benchmark component. The simulation output delineated the stress–strain curves within the linear regime, from which the slopes were used to calculate E_X and E_Y. Modal simulation results validated the first resonant frequency and detailed the mode shapes—bending, twisting, and lead–lag—enhancing the accuracy of the Y-direction predictions.

This initial tensile simulation is crucial in setting a range of input values for lamina property predictions in subsequent stages and in affirming the predicted lamina properties through cross-verification.

3.2. Prediction of E_1 and E_2 of a Lamina and the Optimum Stacking Design

The elastic moduli E_1 and E_2 were prognosticated utilizing the direct optimization feature in ANSYS, informed by tensile and modal simulation data. To streamline computational efforts, a specific range of input data was chosen to ensure the acquisition of valid E_X and E_Y values based on the elastic modulus values of the laminate composites. In the specific range, E_1 and E_2, which can produce E_x and E_y of the laminated composite considering the stacking sequence, were excluded from the range. The inverse prediction calculations harnessed the capabilities of the multi-objective genetic algorithm (MOGA) within the direct optimization tool, which was employed to minimize discrepancies in the elastic modulus of the lamina during the iterative calculation sequence.

Within the MOGA framework, the starting sample size was set at 20, incrementally increasing by 10 with each iteration, with an upper limit of 20 iterations. The algorithmic repetition ceased once the stress and strain were computed in the tensile simulations, using the estimated values of E_1 and E_2 for the lamina aligned with the predefined target stress and strain values. Another condition for termination was the equivalence between the simulation's stress–strain output and the actual tensile test results from the specimen of the structure under analysis. The selection of the initial simulation for subsequent iterative simulations was automated.

From the diverse combinations of predicted E_1 and E_2 values, the pair that yielded simulation results matching the target stress and strain was chosen. The validity of this result was confirmed by comparing the predicted E_X and E_Y (derived from the optimal E_1 and E_2 combination) against the actual composite's E_X and E_Y—those calculated using the initially inputted physical properties.

3.3. Coupon Test Simulation with Errors of Fabrication

To underscore the criticality of precise E_2 prediction, a tensile test incorporating manufacturing discrepancies was simulated in Digimat 2020, a commercial software specialized for composite material simulation. This approach aligns with the study's initial intent to establish a simulation-based procedure capable of reducing the reliance on actual composite material testing, which traditionally incurs substantial experimental costs.

4. Results and Discussion

4.1. Validation of Simulation Procedures for Predicting Lamina Properties

The algorithm for the proposed inverse calculation simulation aimed at predicting the elastic modulus of lamina within laminated composites was corroborated using two distinct methods. The initial method involved the replication of the simulation process with the use of generalized and arbitrary lamina properties. The validity of the predicted lamina properties was ascertained by comparing the simulation outcomes with the initially inputted properties.

The alternative method implemented a simulation with the laminated composite properties derived from the experimental data cited in reference [15]. Here, the accuracy was gauged by juxtaposing the simulated lamina properties against those obtained from the CLPT-based reference study.

For the first method, the reverse-engineering feasibility for CFRP laminae from CFRP-laminated composites was demonstrated using a hypothetical model of four laminated CFRP prepreg sheets. The tensile and modal simulations were conducted with general CFRP properties and a random stack sequence, as detailed in Table 1, adhering to the simulation protocol established in this research. Notably, the first-step simulation excluded properties related to failure modes, since the focus was solely on the elastic domain. The stress–strain curve (S-S curve) was generated from the stresses and strains computed upon applying a 0.3 mm deformation in the tensile direction to the specimen.

Given the simulation's minimum time step of 1 s and the standard test condition of a 2 mm/min deformation rate, a strain rate of 0.3 mm/s was employed. The resulting S-S curve, E_X, and E_Y were extracted from the simulation outputs, as illustrated in Figure 4.

Table 1. Inputs of a case in the tensile simulation and modal simulation for calculating E_X and E_Y.

Material Type	CFRP UD Prepreg
Stacking sequence	[0/90] s
Thickness of one lamina	0.15 mm
Dimension of specimen	13 × 240 mm
E_1 of one lamina	140 GPa
E_2 of one lamina	8.4 GPa
G_{12} of one lamina	4.5 GPa
G_{23} of one lamina	3.5 GPa
Poisson's $ratio_{12}$ of one lamina	0.281
Poisson's $ratio_{23}$ of one lamina	0.4
Node	1098
Elements	963

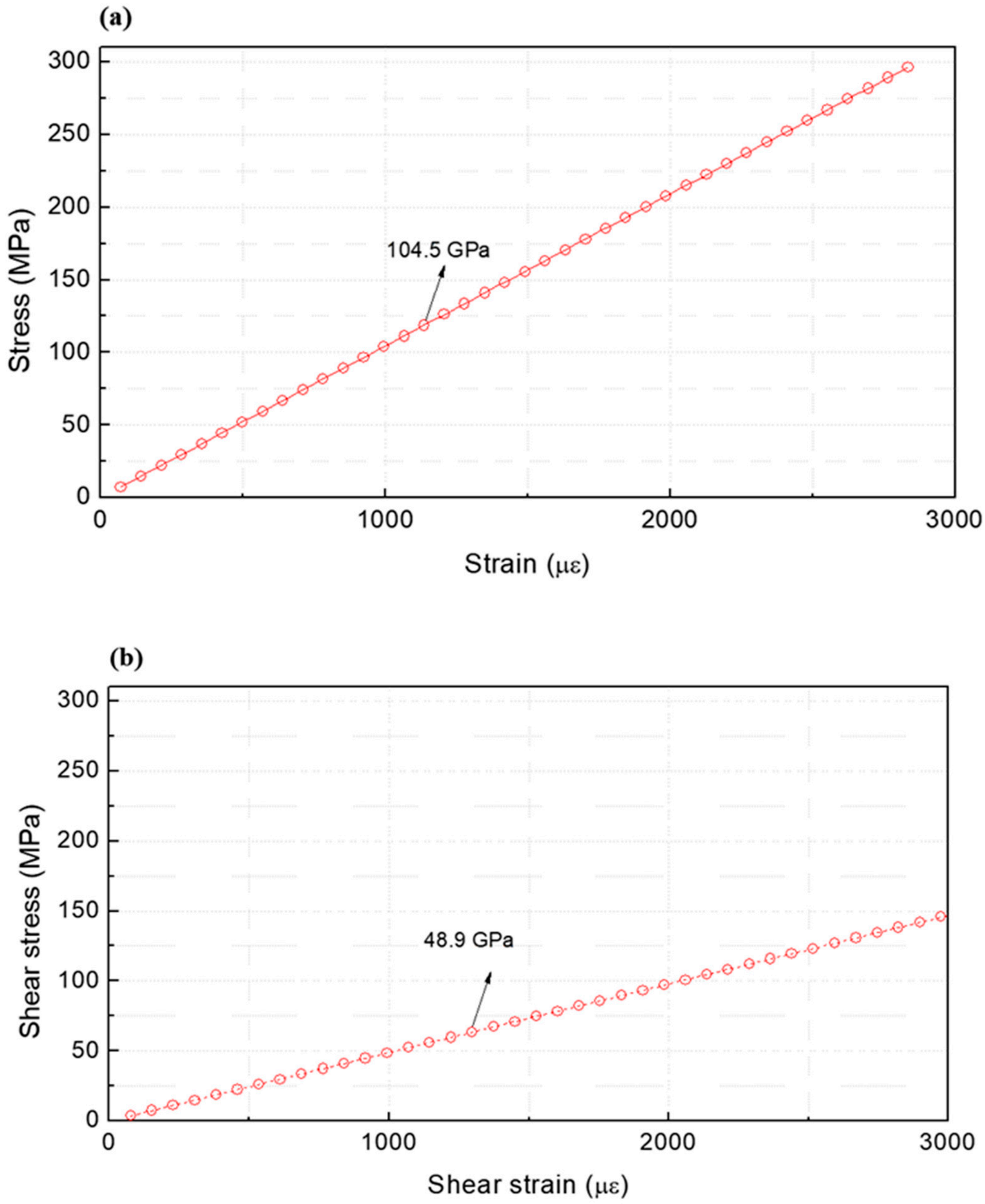

Figure 4. (**a**) E_X and (**b**) E_Y of the laminated composite predicted from the slope of the S-S curve obtained via tensile simulation.

The subsequent phase entailed predicting E_1 and E_2, with the corresponding results presented in Table 2. The selection of target stress and strain values for the inverse calculation was informed by the tensile and modal simulation outcomes of E_X and E_Y. Utilizing the MOGA algorithm and iterative cycles, the optimal E_1 and E_2 combinations were deduced, aiming to closely match the predicted stresses and strains of the laminate composites with the target values, as depicted in Figure 5. The preferred combinations of the predicted E_1 and E_2, tailored to the cases within the repetition loop, are documented in Tables 3 and 4, respectively.

Table 2. Inputs of a case in the simulation of prediction of E_1 and E_2.

Material Type	CFRP UD Prepreg
Stacking sequence	[0/90] s
Thickness of one lamina	0.15 mm
Dimension of specimen	13 × 240 mm
Boundary of E_1 of one lamina	117 GPa < E_1 < 144 GPa
Boundary of E_2 of one lamina	7.68 GPa < E_2 < 9.02 GPa
Stress value to be obtained by inverse calculation	296.54 MPa
Strain value to be obtained by inverse calculation	0.00284 mm/mm
The optimization tool used	MOGA

Table 3. Estimated E_1, E_2 of the simulation in the static condition (tensile condition).

	Initial Input Values	Candidate 1	Candidate 2	Candidate 3
E_1 of lamina (GPa) (Error %)	140.49	140.93 (0.31%)	142.14 (1.17%)	140.83 (0.24%)
E_2 of lamina (GPa) (Error %)	8.49	7.47 (12.01%)	7.88 (7.18%)	8.29 (2.35%)
Simulated stress of the composite (MPa) (Error %)	296.54	297.32 (0.26%)	299.98 (1.16%)	297.23 (0.23%)

Table 4. E_1, E_2 estimated in the simulation in the static (tensile) and dynamic (bending + torsion + lead–lag) conditions.

	Initial Input Values	Candidate 1	Candidate 2	Candidate 3
E_1 of lamina (GPa) (Error %)	140.49	140.63 (0.09%)	140.89 (0.28%)	140.83 (0.24%)
E_2 of lamina (GPa) (Error %)	8.49	8.18 (3.65%)	7.87 (7.30%)	8.90 (4.82%)
Simulated stress of the composite (MPa) (Error %)	296.54	296.79 (0.08%)	297.3 (0.25%)	297.33 (0.26%)
1st Bending frequency (Hz) (Error %)	28.79	28.8 (0.03%)	28.82 (0.1%)	28.83 (0.13%)
1st Torsion frequency (Hz) (Error %)	222.55	222.55 (0%)	222.56 (0.004%)	222.57 (0.008%)
1st Lead–lag frequency (Hz) (Error %)	543.35	543.05 (0.005%)	542.93 (0.007%)	544.67 (0.24%)

The juxtaposition of the results in Tables 3 and 4 underscores the importance of incorporating dynamic characteristics in the inverse calculations. These tables illustrate the discrepancies, termed as errors, between the predicted E_1 and E_2 and the initial input values (reflecting the experimentally measured values under general conditions). Figure 6 visually represents the variance in errors across selected simulation cases.

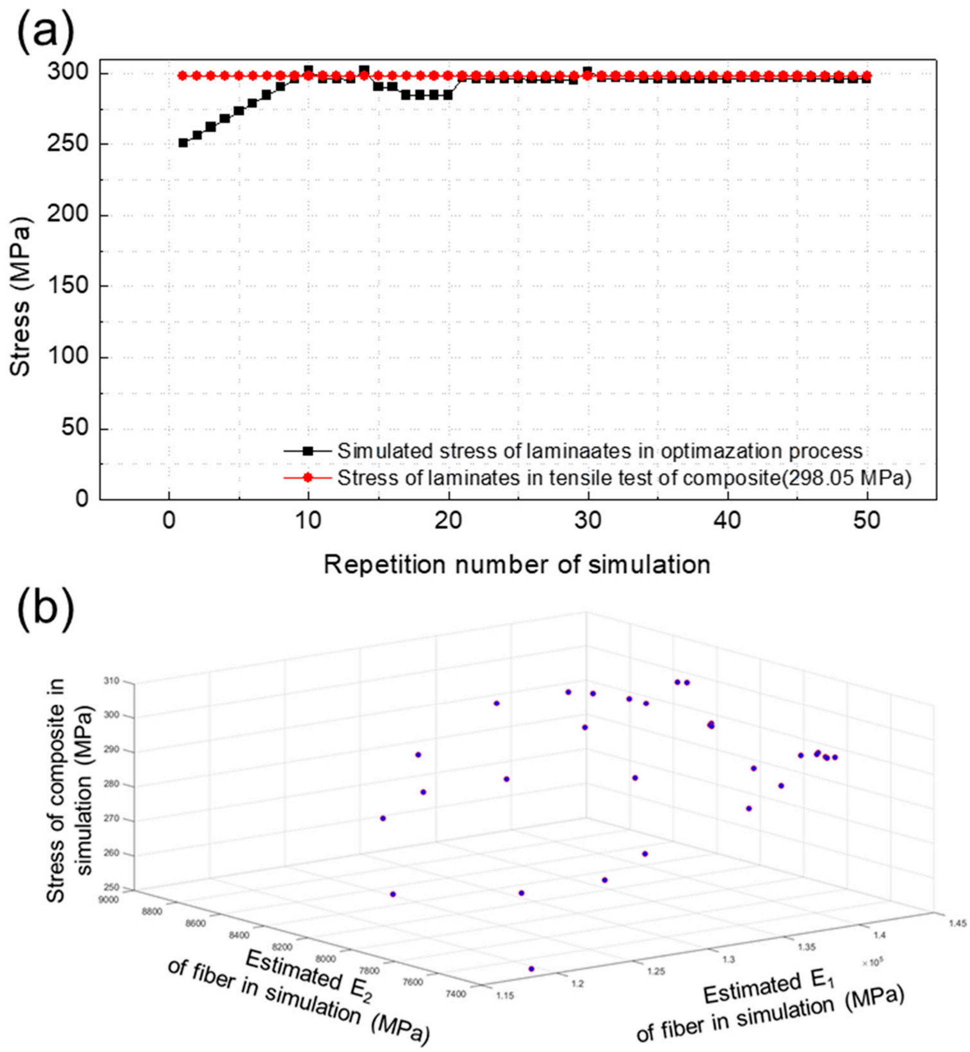

Figure 5. (**a**) Stresses of the laminated composites calculated based on the predicted elastic modulus components (E_1 and E_2) for the approximation to the target values; (**b**) E_1, E_2 combinations calculated using genetic algorithms and iterative loops.

Table 3 details the optimal predicted lamina properties derived from tensile simulation parameters. In this context, Table 3 (Case #1 in Figure 6) exhibits errors for E_1 and E_2 ranging between 0.24 and 1.17%, and 2.35 and 12.01%, respectively. Moreover, a nuanced observation reveals that while Table 3—Candidate 1 presents a larger E_2 error (12.01%) compared to Table 3—Candidate 2's E_2 error (7.18%), the stress error in Candidate 1 (0.26%) is lower than that in Candidate 2 (1.16%). This discrepancy arises because the elastic modulus in the fiber direction (E_1) has a more significant impact on the laminated composite than the modulus in the matrix direction (E_2). Consequently, even a relatively large error in E_2 does not substantially affect the stress prediction accuracy, given that the model consists solely of unidirectional (UD) prepregs, making E_1 the predominant factor.

However, the precise estimation of E_2 assumes critical importance in reverse engineering, especially when considering varied operational conditions. Thus, the dynamic characteristics of the modal test simulation were integrated into the workflow to minimize the predictive error of E_2. Table 4 (Case #4 in Figure 6) displays the improved predictions when dynamic factors—such as the first frequency indicative of bending, torsion, and lead–lag—are included in the tensile simulation. Here, the error margins for E_1 and E_2 are significantly narrowed to 0.09–0.24% and 3.65–7.30%, respectively. The maximal error for E_2 between Tables 3 and 4 reduces from 12.01% to 7.30%, evidencing the benefit of considering dynamic characteristics.

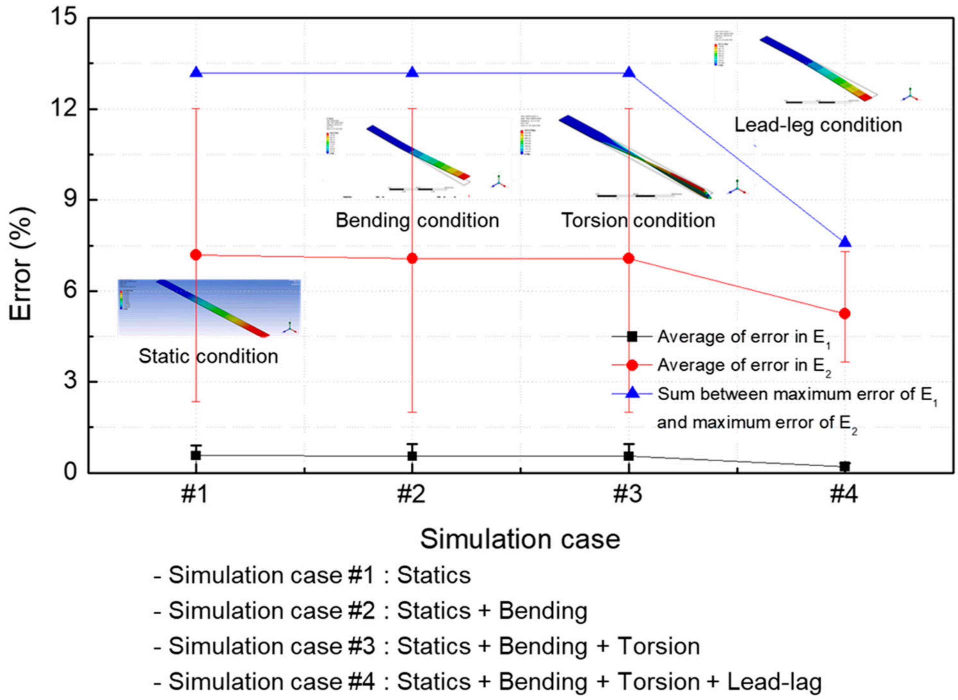

Figure 6. Comparison of the errors between the simulation cases selected.

The improved prediction accuracy in Table 4 stems from cases that significantly influence the properties in the fiber direction. To further evaluate the accuracy of E_2 prediction, simulations on laminated composites with woven fabrics were conducted; the methodology and findings are elaborated in the subsequent section.

In the second verification method, this study's process was validated against the CLPT-based prediction method outcomes detailed in reference [15]. The experimental data and lamination details crucial for reverse engineering are outlined in Table 5. An FEM model deformation was implemented to yield a strain of 3000 microstrains (με), aligning with ASTM D3039's recommended range for modulus-of-elasticity assessment. For authenticity, the specimen's central point was designated for strain measurement, as depicted in Figure 7. Additionally, as shown in Figure 7, 3D modeling was created considering the actual stacking sequence, lamina thickness, and specimen size used in reference [13]. The predicted stress–strain (S–S) curve and the E_X for the laminate are demonstrated in Figure 8, with a noted error margin of 3.75% between the predicted and experimental outcomes, suggesting reliable simulation results.

Table 5. Experimental data used in ref. [15] and stacking information for the reverse design (material, stacking angle, layer thickness, strain, and stress).

Material Type	CFRP UD Prepreg, CFRP Woven Prepreg
Stacking sequence	[±45/0] s
Thickness of one lamina	UD: 0.327 mm, Woven: 0.223 mm
Dimensions of specimen	13 × 240 mm
Measured stress at strain of 3000 με	200 MPa

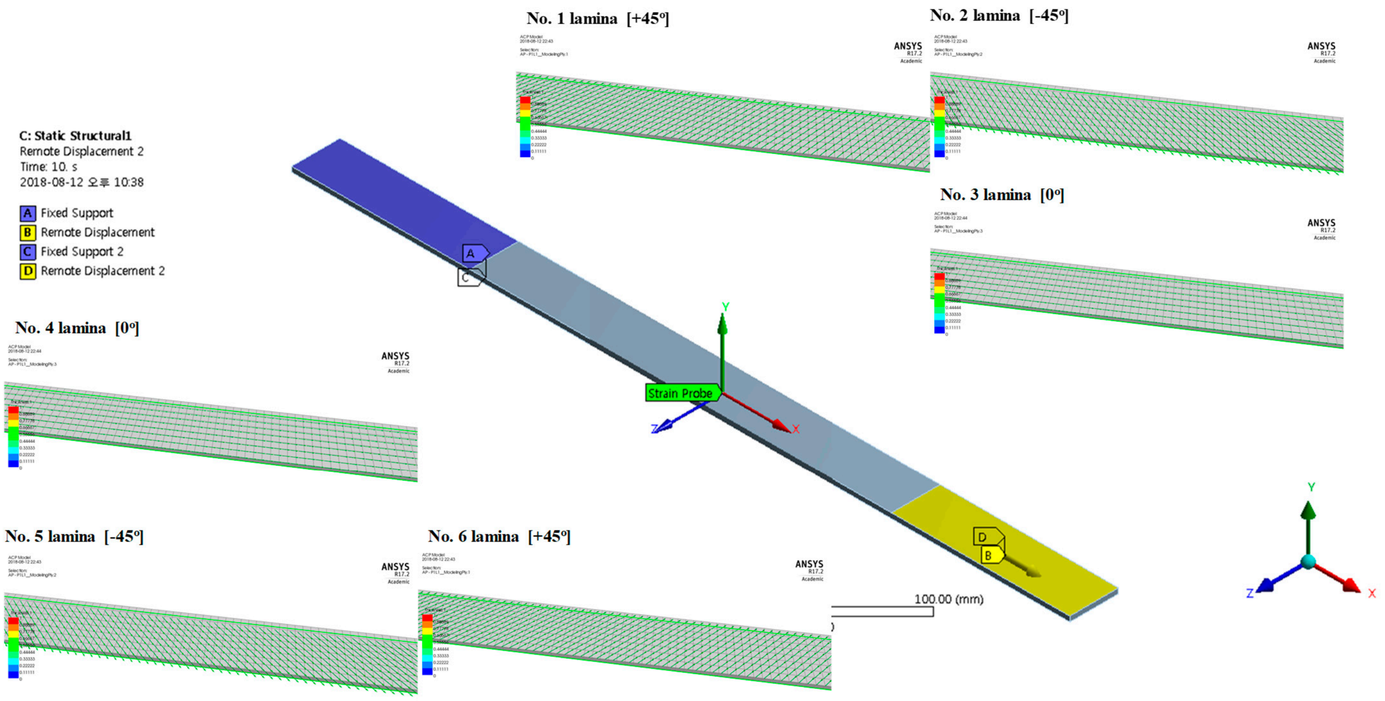

Figure 7. Case in tensile simulation for calculating E_X and E_Y considering the measured point of strain and the stacking information.

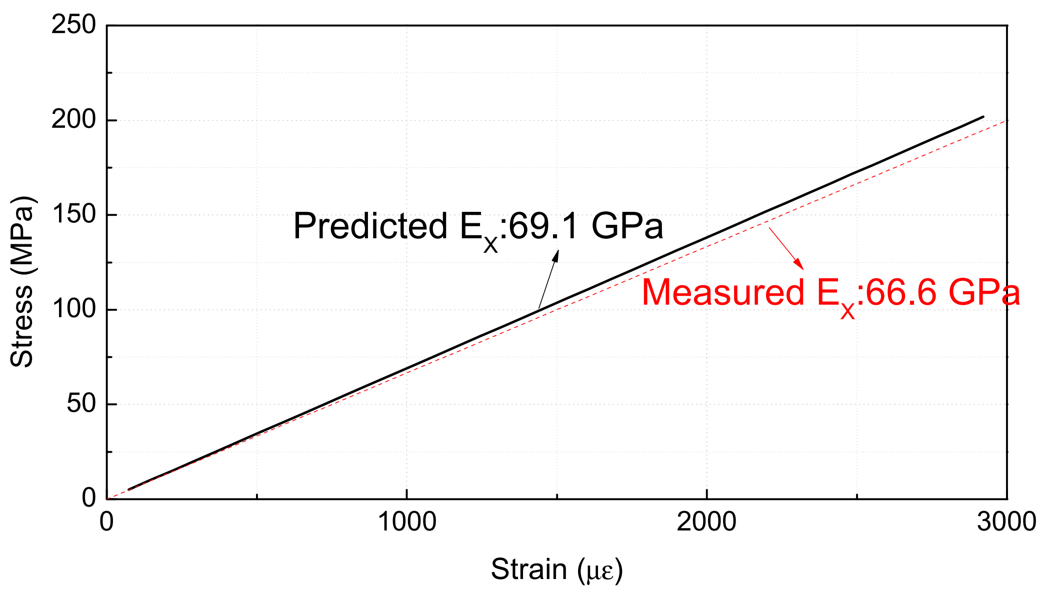

Figure 8. Strain–stress curve of laminated composites and the E_X of the laminated composite calculated from the slope of the curve.

Table 6 presents the lamina properties as predicted using this study's proposed method, the CLPT-based process, and the actual tensile test results from [15]. The first line of Table 6 presents the tensile test results for lamina samples made from a fiber type estimated via the CLPT method. The experimental figures for E_1 and E_2 stood at 109 GPa and 7.8 GPa, respectively, while the simulation method delivered E_1 and E_2 values of 100.13 GPa and 7.3 GPa. Both the simulation and CLPT-based methods yielded comparable errors for E_1 (8.1% and 7.3%, respectively), but the simulation method reported a lower error for E_2 (6.4%) than the CLPT-based method.

Table 6. The predicted lamina properties and the errors between the predicted lamina properties and the experimental results in [13].

	E_1 of UD Lamina (GPa) (Error %)	E_2 of UD Lamina (GPa) (Error %)	E_1 of Woven Lamina (GPa)
Experimental results in [15]	109 GPa	7.8 GPa	Not measured
Properties predicted via the proposed method	100.13 GPa (8.1%)	7.3 GPa (6.4%)	45.56 GPa
Predicted properties based on CLPT in [15]	117 GPa (7.3%)	6.9 GPa (11.5%)	Cannot predict

A notable distinction of the proposed method is its capability to predict properties of woven laminae, a task unattainable through the CLPT-based prediction approach. The FEM-based simulation incorporated in the proposed method enables this broader predictive scope. This study confirmed the viability of obtaining lamina elastic moduli for reverse engineering via this simulation approach.

Errors in the predictive outcomes were attributed to production flaws and testing limitations, considering that the tensile test specimen was created using fibers determined based on the prediction. The proposed method offers a significant advantage—it reduces the necessity for extensive testing compared to traditional inverse calculation methods. It enables the prediction of lamina properties through tensile tests on specimens derived from finished parts. Conversely, CLPT-based reverse calculations mandate at least two tensile tests: one along the fiber direction and another perpendicular to it. Thus, subsequent sections of this study introduce a methodology that accounts for manufacturing and experimental inaccuracies.

4.2. Validation of Coupon Test Simulation with Errors of Fabrication

This study aimed to simulate the elastic modulus range in a laminated composite using laminae with previously predicted properties. The commercial software Digimat-VA 2020 was employed to forecast feasible ranges of values based on the simulations conducted in prior steps, as illustrated in Figure 9. Figure 9 shows the iterative tensile simulation procedure and information considering the test environment variables using E_1 and E_2 predicted from the simulation procedure performed in Section 4.1 for verification purposes. To corroborate the simulation method, specimens were produced using CFRP grades that closely matched the predicted physical characteristics, and tensile tests were performed on these samples.

The previous step's predictions were used to infer the properties of the laminae. In reference [15], these predicted lamina properties were employed to approximate the properties of fibers within laminae of similar grades. A discrepancy arose because the modulus of the resin was not taken into account. Consequently, the moduli of both the fiber and resin were inversely deduced from the predicted lamina modulus through the homogenization method, and these findings are compiled in Table 7.

Table 7. The physical properties of the fibers and resin inversely calculated using the homogenization method.

Input Properties of the Predicted Lamina		Calculated Properties	
E_1 of lamina (MPa)	140,000	E of carbon fiber (MPa)	230,000
E_2 of lamina (MPa)	8200	E of resin (MPa)	4000
Volume fraction of lamina (%)	60%		

Despite the precision of the predictions regarding the stiffness of the fibers, discrepancies in actual testing can arise due to material variations, manufacturing processes, and the testing equipment itself. Therefore, the predicted fibers and resins were utilized to construct a finite element model that mirrored the one employed in the actual tests. Information on lamination order and geometry, akin to that derived from tensile simulations, was integrated into this model. A series of iterative simulations were then executed in batches, considering a spectrum of potential variables. Table 8 details the varied conditions for the coupon test simulations that included a fabrication tolerance.

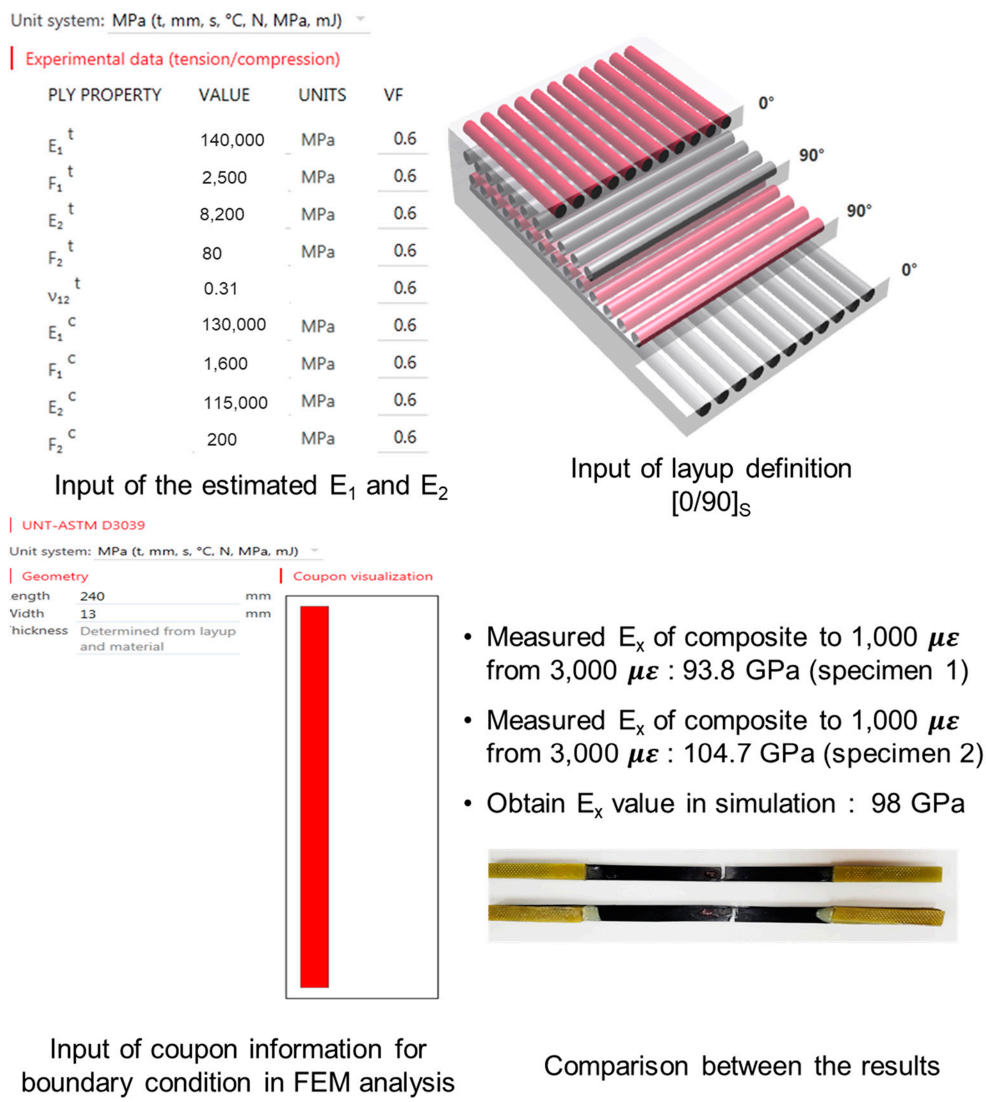

Figure 9. Coupon specimen test simulation with statistical simulation based on the predicted laminae properties.

Table 8. Variable condition of coupon test simulation; the predicted elastic modulus and strength are calculated based on the following conditions.

Allowance Type	Condition
Material variability	Matrix tensile strength ±5% Fiber tensile strength ±5%
Process variability	Fiber volume fraction ±10% Ply misalignment standard deviation ±3°
Experimental variability	Coupon misalignment standard deviation ±3

The statistical analysis of repeated simulations, presented in Figure 10, showcased the distribution of elastic modulus values for a composite laminate modeled as [0/90] s. The A-basis and B-basis values were utilized as statistical measures to indicate the confidence levels and reliability of the data. Specifically, the A-basis value represented the lower bound of the elastic modulus, with 99% of the data expected to exceed this value at a 95% confidence level. The B-basis was less stringent, with 90% of the data exceeding the basis value at the same confidence level.

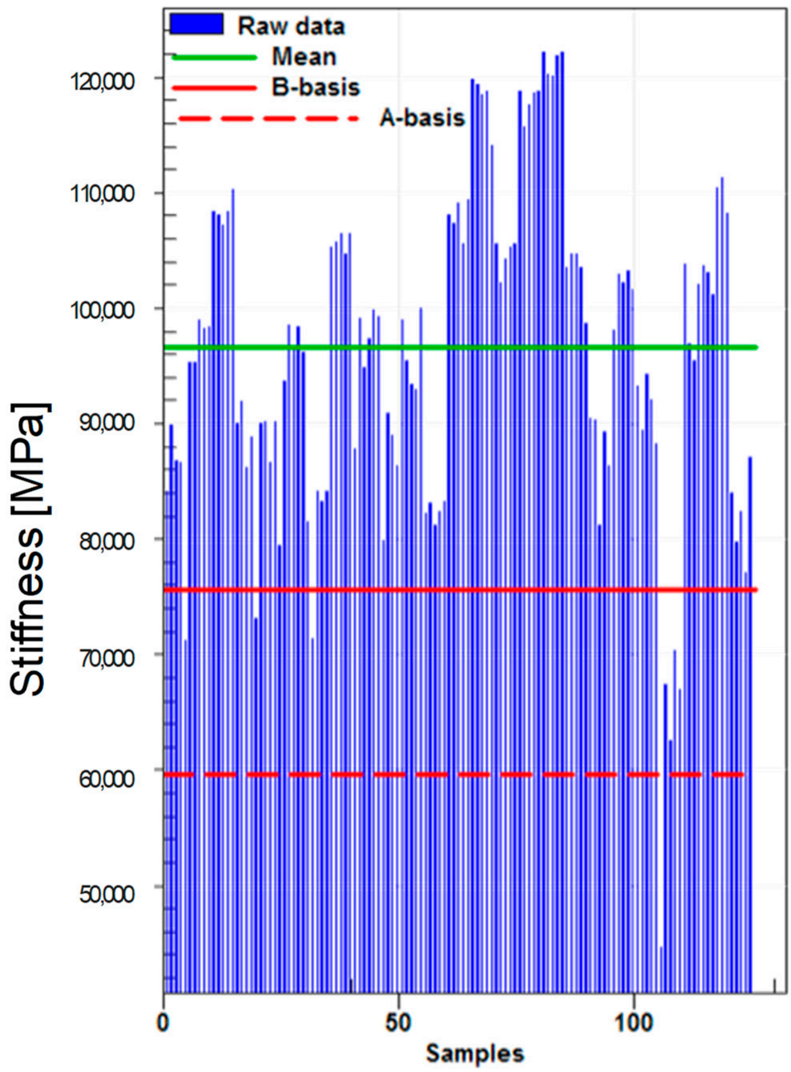

Figure 10. Coupon test simulation results according to allowance variables.

In 125 simulation cases, the lowest E_X value of the laminated composite dropped to 59 GPa at an A-basis reliability level due to variability in fabrication conditions. However, at the B-basis level (90% confidence), the lowest E_X value was higher, at 75 GPa. The simulated E_X value from the prior step was 98 GPa, while the actual experimental results for two produced specimens yielded E_X values of 93.8 GPa and 104.7 GPa, respectively. These findings confirmed the appropriateness of the simulation process.

A further analysis was conducted using the surface response method, detailed in Figure 11, which examined the interaction between various factors influencing the composite's strength. The central synthesis method among response surface methods, as shown in Figure 11, was used to analyze the relationship between test parameters related to coupon test simulation. After analyzing the relationship between factors interacting based on composite stiffness, sensitivity was calculated using the sensitivity calculation method in reference [30]. As shown in Table 9, because the sensitivity of the matrix tensile strength is the greatest, it was found to have the greatest influence on the analysis results. This analysis pinpointed the matrix tensile strength as the most significant contributing factor to the overall strength properties of the laminated composite material.

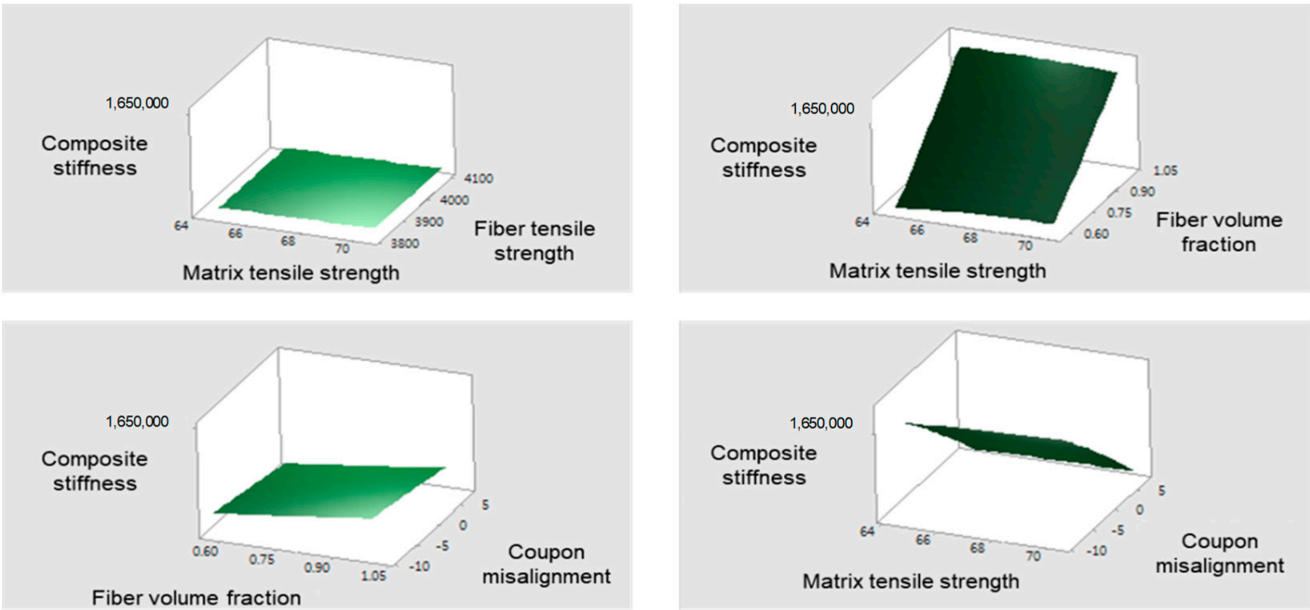

Figure 11. Coupon test simulation results analyzed using a surface reaction method.

Table 9. Sensitivity of allowance variables in the repeated simulations.

Material Type	Sensitivity
Matrix tensile strength	9.63×10^{-1}
Fiber volume fraction	1.42×10^{-2}
Fiber tensile strength	1.74×10^{-2}
Coupon misalignment	5.13×10^{-3}

Simulations that factored in manufacturing errors underscored the criticality of precisely analyzing E_2, the modulus of elasticity in the transverse direction of the lamina. The methodology proposed in this study proved itself capable of predicting E_2 with a lower margin of error, thereby enhancing the reliability of the simulation outcomes for the composite's performance under varied manufacturing conditions.

5. Conclusions

A novel reverse-design methodology and simulation process were developed to accurately determine the elastic modulus of the fiber layers in laminated composites. This process is unique in that it can effectively calculate both longitudinal and transverse elastic moduli by utilizing both static and dynamic simulation results of the structural behavior.

The procedure involved modeling the shape of the composite material in ANSYS PrePost, considering the stacking information, and employing tensile simulation and modal analysis to determine E_X and E_Y. The elastic moduli, E_1 and E_2, were predicted using an MOGA within an iterative calculation framework. The accuracy of this predictive algorithm improved significantly when both static (tensile) and dynamic (modal) characteristics were incorporated. The error in stress prediction for the laminated composite was minimized to 0.08% when both simulation results were used, highlighting the effectiveness of the combined simulation approach.

This study also demonstrated that the error margin for predicting E_1 and E_2 was considerably reduced when both static and dynamic results were considered. The error ranges for E_1 were reduced to 0.09–0.24% and for E_2 to 3.65–7.30%. The prediction error for E_2 was notably decreased when lead–lag resonance information was included, emphasizing the importance of dynamic simulation for accurately assessing the stiffness in lateral motion.

Simulations that accounted for fabrication tolerances underscored the necessity of precisely analyzing E_2, with the proposed method showing a lower error for E_2. This indicates that the simulation approach can effectively account for manufacturing variabilities.

Ultimately, this study confirmed the feasibility of reverse engineering laminated composites and improving the precision of such processes. The method developed provides a potent tool for estimating lamina information in unknown laminated composite structures, which could be highly beneficial for the field of composite material design.

Author Contributions: Conceptualization, M.-Y.H. and H.C.L.; methodology, M.-Y.H.; software, M.-Y.H.; validation, M.-Y.H.; investigation, J.H.P.; data curation, J.H.P.; writing—original draft preparation, M.-Y.H.; writing—review and editing, M.-Y.H. and H.C.L.; project administration, J.S.; funding acquisition, S.W.H. and H.H.K. All authors have read and agreed to the published version of the manuscript.

Funding: This research received no external funding.

Data Availability Statement: All data generated of this work are included in this article.

Acknowledgments: This work was supported by the Automotive Industry Technology Development Program of the Korea Planning and Evaluation Institute of Industrial Technology (KEIT). It was granted financial resources from the Ministry of Trade, Industry & Energy, Republic of Korea. (Development of a vehicle floor carpet product with more than 90% antiviral function using recycled PET coating fabric, No. 20018915.)

Conflicts of Interest: The authors declare no conflict of interest. Soo Woong Hwang is an employee of Moodng Co., Ltd. and Hun Hee Kang is an employee of NK Alkenz Co., Ltd. The paper reflects the views of the scientists, and not the companies.

References

1. Shokrieh, M.M.; Rezaei, D. Analysis and optimization of a composite leaf spring. *Compos. Struct.* **2003**, *60*, 317–325. [CrossRef]
2. Choi, B.-H.; Lee, J.-B.; Choi, B. A Study on the Hysteresis Characteristics and Finite Element Analysis of FRP Leaf Spring. *J. Adv. Eng. Technol.* **2009**, *2*, 291–298. Available online: https://kiss.kstudy.com/Detail/Ar?key=3346071 (accessed on 1 June 2023).
3. Kim, C.-S.; Park, S.-Y. Diesel engine intake port analysis using reverse-engineering technique. *Trans. Korean Soc. Automot. Eng.* **2015**, *23*, 502–507. [CrossRef]
4. Roos, T.H.; Quin, R.L.; De Beer, F.C.; Nshimirimana, R.M. Neutron tomography as a reverse engineering method applied to the IS-60 Rover gas turbine. *Nucl. Instrum. Methods Phys. Res. A* **2011**, *651*, 329–335. [CrossRef]
5. Dúbravčík, M.; Kender, Š. Application of reverse engineering techniques in mechanics system services. *Procedia Eng.* **2012**, *48*, 96–104. [CrossRef]
6. Gameros, A.; De Chiffre, L.; Siller, H.R.; Hiller, J.; Genta, G. A reverse engineering methodology for nickel alloy turbine blades with internal features. *CIRP J. Manuf. Sci. Technol.* **2015**, *9*, 116–124. [CrossRef]
7. Oh, S.; Chang, B.; Ro, Y. A study on the appropriateness of virtual machine for reverse engineering. *Trans. Korean Soc. Automot. Eng.* **2014**, *22*, 31–38. [CrossRef]
8. Jang, A.; Jeong, S.; Park, M.J.; Ju, Y.K. Structural evaluation by reverse engineering with 3D laser scanner. *ce/papers* **2023**, *6*, 308–314. [CrossRef]
9. Kim, Y.-W.; Kim, J.-H.; Jeong, K.-S. Crash FE analysis of front side assembly for reverse engineering. *Trans. Korean Soc. Automot. Eng.* **2007**, *15*, 89–98.
10. Cumbo, R.; Baroni, A.; Ricciardi, A.; Corvaglia, S. Design allowables of composite laminates: A review. *J. Compos. Mater.* **2022**, *56*, 3617–3634. [CrossRef]
11. Carlsson, L.A.; Adams, D.F.; Pipes, R.B. *Experimental Characterization of Advanced Composite Materials*; CRC Press: Boca Raton, FL, USA, 2014.
12. Maurin, R.; Davies, P.; Baral, N.; Baley, C. Transverse properties of carbon fibres by nano-indentation and micro-mechanics. *Appl. Compos. Mater.* **2008**, *15*, 61–73. [CrossRef]
13. *ASTM D3379*; Standard Test Method for Tensile Strength and Young's Modulus for High-Modulus Single-Filament Materials. ASTM International: Conshohocken, PA, USA, 1989.
14. *ASTM D638-14*; Standard Test Method for Tensile Properties of Plastics. ASTM International: Conshohocken, PA, USA, 2014.
15. Moon, J.B.; Kim, J.; Jang, H.K.; Park, J. A study on calculation of composites lamina material properties through reverse engineering of light weight composite car-body. *Trans. Korean Soc. Automot. Eng.* **2017**, *25*, 1–10. [CrossRef]
16. Hwang, Y.-T.; Lim, J.-Y.; Nam, B.-G.; Kim, H.-S. Analytical prediction and validation of elastic behavior of carbon-fiber-reinforced woven composites. *Compos. Res.* **2018**, *31*, 276–281.
17. Gibson, R.F. *Principles of Composite Material Mechanics*; CRC Press: Boca Raton, FL, USA, 2016.

18. Li, X.; Guan, Z.; Li, Z.; Liu, L. A new stress-based multi-scale failure criterion of composites and its validation in open hole tension tests. *Chin. J. Aeronaut.* **2014**, *27*, 1430–1441. [CrossRef]
19. Vanaerschot, A.; Cox, B.N.; Lomov, S.V.; Vandepitte, D. Multi-scale modelling strategy for textile composites based on stochastic reinforcement geometry. *Comput. Methods Appl. Mech. Eng.* **2016**, *310*, 906–934. [CrossRef]
20. Furtado, S.C.R.; Araújo, A.L.; Silva, A. Inverse characterization of vegetable fibre-reinforced composites exposed to environmental degradation. *Compos. Struct.* **2018**, *189*, 529–544. [CrossRef]
21. Zhou, X.-Y.; Gosling, P.D.; Ullah, Z.; Kaczmarczyk, Ł.; Pearce, C.J. Exploiting the benefits of multi-scale analysis in reliability analysis for composite structures. *Compos. Struct.* **2016**, *155*, 197–212. [CrossRef]
22. Voyiadjis, G.Z.; Kattan, P.I. *Mechanics of Composite Materials with MATLAB*; Springer Science and Business Media: Berlin/Heidelberg, Germany, 2005.
23. Reddy, J.N. *Mechanics of Laminated Composite Plates and Shells: Theory and Analysis*; CRC Press: Boca Raton, FL, USA, 2003.
24. Chia, C.-Y. *Nonlinear Analysis of Plates*; McGraw-Hill International Book Company: New York, NY, USA, 1980.
25. Ribeiro, P. A hierarchical finite element for geometrically non-linear vibration of doubly curved, moderately thick isotropic shallow shells. *Int. J. Numer. Methods Eng.* **2003**, *56*, 715–738. [CrossRef]
26. Akhavan, H.; Ribeiro, P. Natural modes of vibration of variable stiffness composite laminates with curvilinear fibers. *Compos. Struct.* **2011**, *93*, 3040–3047. [CrossRef]
27. Zebdi, O.; Boukhili, R.; Trochu, F. An inverse approach based on laminate theory to calculate the mechanical properties of braided composites. *J. Reinf. Plast. Compos.* **2009**, *28*, 2911–2930. [CrossRef]
28. Sztefek, P.; Olsson, R. Nonlinear compressive stiffness in impacted composite laminates determined by an inverse method. *Compos. A* **2009**, *40*, 260–272. [CrossRef]
29. *ASTM D3039*; Standard Test Method for Tensile Properties of Polymer Matrix Composite Materials. ASTM International: Singapore, 2007.
30. Liu, H.; Chen, W.; Sudjianto, A. Probabilistic Sensitivity Analysis Methods for Design under Uncertainty. In Proceedings of the 10th AIAA/ISSMO Multidisciplinary Analysis and Optimization Conference, New York, NY, USA, 30 August–1 September 2004; p. 4589.

Disclaimer/Publisher's Note: The statements, opinions and data contained in all publications are solely those of the individual author(s) and contributor(s) and not of MDPI and/or the editor(s). MDPI and/or the editor(s) disclaim responsibility for any injury to people or property resulting from any ideas, methods, instructions or products referred to in the content.